High sensitivity 10Gb/s Si photonic receiver based on a low-voltage waveguide-coupled Ge avalanche photodetector

H. T. Chen,[1,2,*] J. Verbist,[3] P. Verheyen,[1] P. De Heyn,[1] G. Lepage,[1] J. De Coster,[1] P. Absil,[1] X. Yin,[3] J. Bauwelinck,[3] J. Van Campenhout,[1] and G. Roelkens[2]

[1]IMEC, Kapeldreef 75, Leuven, Belgium
[2]Photonics Research Group, Department of Information Technology, Ghent University - imec, Ghent B-9000, Belgium
[3]Ghent University, INTEC/IMEC, Sint-Pietersnieuwstraat 41, 9000 Gent, Belgium
[*]Hongtao.Chen@imec.be

Abstract: We demonstrate low-voltage germanium waveguide avalanche photodetectors (APDs) with a gain × bandwidth product above 100GHz. A photonic receiver based on such a Ge APD, including a 0.13µm SiGe BiCMOS low-noise trans-impedance amplifier and a limiting amplifier, is realized. A 5.8dB sensitivity improvement is demonstrated at −5.9V bias at an avalanche gain of 6 through bit error ratio measurements. The absolute sensitivity in avalanche mode is −23.4dBm and −24.4dBm at a bit error ratio of 1×10^{-12} and 1×10^{-9} respectively.

OCIS codes: (040.1345) Avalanche photodiodes (APDs); (040.5160) Photodetectors; (200.4650) Optical interconnects.

References and links

1. J. C. Campbell, "Recent advances in telecommunications avalanche photodiodes," J. Lightwave Technol. **25**(1), 109–121 (2007).
2. T. P. Pearsall, H. Temkyn, J. C. Bean, and S. Luryi, "Avalanche gain in GeSi/Si infrared waveguide detectors," Electron. Device Lett. **7**(5), 330–332 (1986).
3. H. Melchior and W. T. Lynch, "Signal and noise response of high-speed germanium avalanche photodiodes," Trans. Electron Devices **13**(12), 829–838 (1966).
4. H. Ando, H. Kanbe, T. Kimura, T. Yamaoka, and T. Kaneda, "Characteristics of germanium avalanche photodiodes in the wavelength region of 1–1.6 µm," J. Quantum Electron. **14**(11), 804–809 (1978).
5. Y. Kang, H. D. Liu, M. Morse, M. J. Paniccia, M. Zadka, S. Litski, G. Sarid, A. Pauchard, Y. H. Kuo, H. W. Chen, W. Sfar Zaoui, J. E. Bowers, A. Beling, D. C. Mcintosh, and J. C. Campbell, "Monolithic germanium/silicon avalanche photodiodes with 340GHz gain-bandwidth product," Nat. Photonics **3**(1), 59–63 (2009).
6. S. Assefa, F. Xia, and Y. A. Vlasov, "Reinventing germanium avalanche photodetector for nanophotonic on-chip optical interconnects," Nature **464**(7285), 80–84 (2010).
7. L. Virot, P. Crozat, J. M. Fédéli, J. M. Hartmann, D. Marris-Morini, E. Cassan, F. Boeuf, and L. Vivien, "Germanium avalanche receiver for low power interconnects," Nat Commun **5**, 4957 (2014).
8. H. T. Chen, P. Verheyen, M. Rakowski, P. De Heyn, G. Lepage, J. De Coster, P. Absil, G. Roelkens, and J. Van Campenhout, "Low-voltage Ge avalanche photodetector for highly sensitive 10Gb/s Si photonic receivers," Proc. 11th International Conference on Group IV Photonics, 106–107 (2014).
9. M. Rakowski, M. Ingels, K. De Meyer, M. Steyaert, P. Absil, and J. Van Campenhout, "Highly sensitive, low-power, 10-20Gb/s transimpedance amplifier based on cascaded CMOS inverter gain stages," Proc. *Optical Interconnects Conference*, 115–116 (2014).
10. X. Yin, J. Put, J. Verbrugghe, J. Gillis, X. Z. Qiu, J. Bauwelinck, J. Vandewege, H. G. Krimmel, and M. Achouche, "A 10Gb/s burst-mode TIA with on-chip reset/lock CM signaling detection and limiting amplifier with a 75ns settling time," IEEE ISSCC Dig. Tech. Papers. 416–417 (2012).
11. X. Yin, X. Z. Qiu, J. Gillis, J. Put, J. Verbrugghe, J. Bauwelinck, J. Vandewege, H. Krimmel, D. van Veen, P. Vetter, and F. Chang, "Experiments on 10Gb/s fast settling high sensitivity burst-mode receiver with on-chip auto-reset for 10G-GPONs [Invited]," JOCN **4**, B68–B76 (2012).
12. M. Pantouvaki, P. Verheyen, G. Lepage, J. De Coster, H. Yu, P. De Heyn, P. Absil, and J. Van Campenhout, "20Gb/s silicon ring modulator co-integrated with a Ge monitor photodetector," ECOC Conference 2013, London, United Kingdom, We.3.B.2.

13. P. De Heyn, J. De Coster, P. Verheyen, G. Lepage, M. Pantouvaki, P. Absil, W. Bogaerts, J. Van Campenhout, and D. Van Thourhout, "Fabrication-tolerant four-channel wavelength-division-multiplexing filter based on collectively tuned Si microrings," J. Lightwave Technol. **31**(16), 2785–2792 (2013).
14. P. Verheyen, M. Pantouvaki, J. Van Campenhout, P. Absil, H. Chen, P. De Heyn, G. Lepage, J. De Coster, P. Dumon, A. Masood, D. Van Thourhout, R. Baets, and W. Bogaerts, "Highly uniform 25 Gb/s Si photonics platform for high-density, low-power WDM optical interconnects," in Advanced Photonics for Communications, OSA Technical Digest (online) (Optical Society of America, 2014), paper IW3A.4.
15. M. M. Hayat, B. E. A. Saleh, and M. C. Teich, "Effect of dead space on gain and noise of double-carrier multiplication avalanche photodiodes," Trans. Electron Devices **39**(3), 546–552 (1992).
16. M. M. Hayat, O. H. Kwon, S. Wang, J. C. Campbell, B. E. A. Saleh, and M. C. Teich, "Boundary effects on multiplication noise in thin heterostructure avalanche photodiodes: theory and experiment," Trans. Electron Devices **49**(12), 2114–2123 (2002).
17. S. C. Liew, C. H. Tan, Y. L. Goh, A. R. Marshall, and J. P. R. David, "Modeling of avalanche multiplication and excess noise factor in InAlAs avalanche photodiodes using a simple Monte Carlo model," J. Appl. Phys. **104**(1), 013114 (2008).
18. R. B. Emmons, "Avalanche-photodiode frequency response," J. Appl. Phys. **38**(9), 3705–3714 (1967).
19. R. J. McIntyre, "The distribution of gains in uniformly multiplying avalanche photodiodes: theory," IEEE Trans. Electron. Dev. **ED-19**(6), 703–713 (1972).
20. W. S. Zaoui, H. W. Chen, J. E. Bowers, Y. Kang, M. Morse, M. J. Paniccia, A. Pauchard, and J. C. Campbell, "Frequency response and bandwidth enhancement in Ge/Si avalanche photodiodes with over 840 GHz gain-bandwidth-product," Opt. Express **17**(15), 12641–12649 (2009).
21. H. T. Chen, P. Verheyen, P. De Heyn, G. Lepage, J. De Coster, P. Absil, G. Roelkens, and J. Van Campenhout, "High responsivity low-voltage 28Gb/s Ge p-i-n photodetector with silicon contacts," J. Lightwave Technol., doi:10.1109/JLT.2014.2367134 (2014).
22. Y. Kang, Z. Huang, Y. Saado, J. Campbell, A. Pauchard, J. Bowers, and M. J. Paniccia, "High performance Ge/Si avalanche photodiodes development in Intel," Proc. Opt. Fiber Commun. **12**, OWZ1 (2011).

1. Introduction

Avalanche photodetectors (APDs) integrated in a silicon photonics platform offer great potential to improve the power budget of Si-based optical interconnects. Moreover, they are potentially disruptive in passive optical access networks requiring high sensitivity at moderate bitrates (10Gbit/s) and low cost. By leveraging the internal gain of the APD, optical receivers can be realized with significantly improved optical sensitivity as compared to conventional PIN photodetector receivers [1]. Multiplication gain and excess noise are key performance metrics for APDs. Although Ge APDs can achieve high gain using carrier multiplication close to avalanche breakdown [2,3], they are generally considered to suffer from the high multiplication noise in germanium [4]. High avalanche gain with low excess noise has been demonstrated in surface normal operating Ge detectors in a Separate Absorption, Charge, and Multiplication (SACM) configuration using Ge as light absorption layer and Si as the multiplication layer [5], enabling an impressive gain-bandwidth product of 340GHz and −28dBm receiver sensitivity at 10Gb/s. However, this implementation requires a high bias voltage of around −25V, which is not compatible with CMOS supply voltages. High avalanche gain at low voltage (−3V) was also reported [6] in waveguide APDs comprised of a thin Ge layer with metal-semiconductor-metal (MSM) contacts. Strongly non-uniform electric fields generated by the interdigitated contacts were exploited to mitigate the intrinsically poor avalanche excess-noise properties of bulk Ge. However, the large dark current of the MSM device and poor primary responsivity strongly limited the receiver sensitivity. Recently, a lateral PIN junction based Ge waveguide APD with gain larger than 10 at a bias voltage of −7V was reported in [7]. The device shows a low dark current of 18nA at −1V. However [7], doesn't demonstrate the sensitivity improvement through bit error rate measurements.

In [8], we demonstrated a 10Gb/s Si photonic receiver based on a low-voltage vertical PIN junction Ge waveguide APD, integrated on the imec 200mm Si photonics platform, wire-bonded to a 40nm LP CMOS trans-impedance amplifier (TIA) [9]. A 7dB receiver sensitivity improvement was estimated based on the Q factor extracted from eye diagram measurements. In this paper, a Ge waveguide APD with a similar design as that in [8] is wire-bonded to a 0.13μm SiGe BiCMOS low-noise TIA [10,11]. Bit error ratio measurements are implemented on the wire-bonded optical receiver to directly access the sensitivity improvement by

operating the Ge APD in the avalanche mode. Also the avalanche noise performance of the Ge APD is characterized by excess multiplication noise measurements.

As for the standalone Ge APD, a 3dB opto-electrical bandwidth above 10GHz at an avalanche gain of 10.2 is obtained at −6.2V, resulting in a gain × bandwidth product (GBP) above 100GHz by leveraging a 400nm thin Ge layer in the vertical PIN structure. It has a low dark current of 17nA at −1V and a high primary responsivity of 0.6A/W. The measured effective ratio of ionization coefficients for electrons and holes (k_{eff}) is as low as 0.5. A significant sensitivity improvement of 5.8dB at −5.9V is demonstrated from bit error ratio measurements on the wire-bonded optical receiver. The primary sensitivity is −17.6dBm and −18.6dBm average optical power (non-return-to-zero modulation at 10Gb/s) at −1.7V for a bit error ratio of 10^{-12} and 10^{-9} respectively. This results in an absolute sensitivity in avalanche mode of −23.4dBm and −24.4dBm at a bit error ratio of 10^{-12} and 10^{-9} respectively.

2. Device structure and fabrication process

The Ge waveguide APDs are implemented in imec's fully integrated Si Photonics Platform along with Si modulators [12] and various passive devices [13]. They go through a process flow described in [14]. The cross-sectional dimensions of the Ge APD are shown in Fig. 1(a). Figure 1(b) shows a TEM image of the Ge APD's longitudinal cross section. The spacing between the p-contact plugs is 1.2µm. With phosphorus ion implantation in silicon before Ge epitaxy and boron ion implantation in the planarized Ge layer, a vertical P^+-I-N^+ (VPIN) diode is formed. The simulated doping distribution (Monte Carlo ion implantation simulation) in the Ge layer is shown in Fig. 1(c). This heterogeneous Ge/Si VPIN diode configuration results in a strong electric field as high as 1×10^5 V·cm^{-1} confined in the lower 200nm of the Ge layer at −5.5V bias voltage, as shown in Fig. 1(d). Hence, it is expected that strong avalanche multiplication can take place at moderate applied bias voltage, and that part of the avalanche excess-noise generation can be suppressed [6, 15–17].
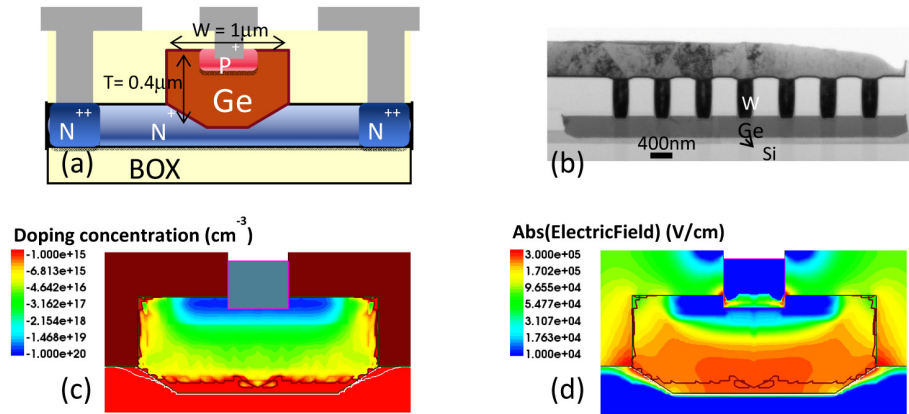

Fig. 1. (a) Schematic cross section of the Ge waveguide APD with the Ge layer dimensions. (b) TEM longitudinal cross-section image. (c) Doping distribution in the Ge layer generated from Monte-Carlo ion implantation simulation. (d) Simulated electric field distribution in the Ge layer at –5.5V applied bias voltage.

3. Standalone APD characteristics

3.1 Static measurements

A typical static current-voltage characteristic of a 14µm-long VPIN Ge APD device is shown in Fig. 2(a). The device has a low dark current of 17nA at −1V. As the bias voltage is increased to −4V, the dark current starts to increase rapidly. The breakdown voltage is −6.2V. The light current is measured at 1550nm wavelength with an input optical power of

−19.6dBm received by the germanium photodiode (using a diffractive grating coupler with −5dB coupling efficiency as fiber-chip interface). The responsivity is constant from 0V to −3V, owing to the relatively large built-in electrical field that is capable of sweeping out the majority of the photo-generated carriers even at 0V bias. The measured primary responsivity is 0.6A/W. The light current is 7µA at −1V. It starts to rise from −4V, and it reaches 260µA at −6.2V.

The avalanche gain extracted from these static measurements, defined as the multiplication factor of the net-light current (= light current – dark current) is shown in Fig. 2(b). The gain increases sharply as the bias voltage becomes larger than −5V, reaching its maximum value at −6.2V. Beyond this breakdown voltage, the gain decreases instead. It can be seen that at 90%, 95% and 98% of the breakdown voltage, the avalanche gain is 3.5, 6.3 and 10.0 respectively. The avalanche gain is independent of input optical power in the range from −30dBm to −15dBm.
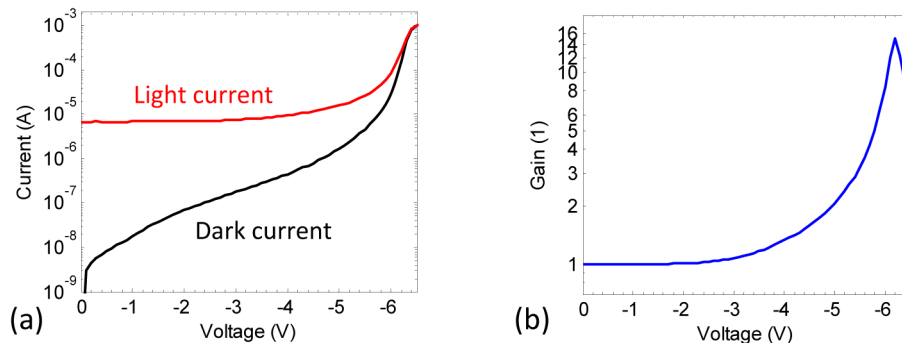

Fig. 2. (a) I-V characteristics of a 14µm-long Ge APD (in the dark and under an input optical power of −19.6dBm). (b) Avalanche gain extracted from the static measurements.

3.2 Small-signal measurements

Next, small-signal radio-frequency (RF) measurements at 1550nm wavelength are carried out. Using an average input optical power of −15.8dBm, the RF power delivered by the photodetector to a vector network analyzer (the S_{21} parameter) is recorded as a function of frequency for various applied bias voltages, as shown in Fig. 3. It can be seen that the low-frequency RF power increases with bias voltage until −6.2V. Beyond this voltage, the low-frequency RF power drops instead, in accordance with the static measurements. Also, it can be seen that the 3dB opto-electrical bandwidth drops substantially with increasing bias voltage.

Avalanche gain extracted from small-signal measurements, defined as the square root of the multiplication factor of the low-frequency RF power (using the low frequency RF power at −1V as a reference), is shown in Fig. 4(a). Similar to what was obtained from the static measurements, the avalanche gain extracted from small-signal measurements reaches its maximum value at −6.2V. Besides, it is independent of input optical power in the range from −30dBm to −15dBm. The 3dB opto-electrical bandwidth versus avalanche gain is shown in Fig. 4(b). At low bias voltages, the 3dB bandwidth is as high as 50GHz (limited by the measurement setup). It decreases slowly as long as the multiplication gain is smaller than 2. As the gain further increases, the 3dB bandwidth drops almost inversely proportional to the avalanche gain owing to the avalanche build-up time [18,19]. At −6.2V APD bias, a 3dB bandwidth of 10.4GHz at the avalanche gain of 10.2 is obtained. The gain × bandwidth product (GBP) is shown in Fig. 3(c). It can be seen that the GBP reaches a plateau at −5.8V (~100GHz), after which it further increases due to bandwidth enhancement as seen in Fig.

3(b), similar to what is reported in [20]. The 100GHz GBP is comparable to standard InP-based APDs [5].
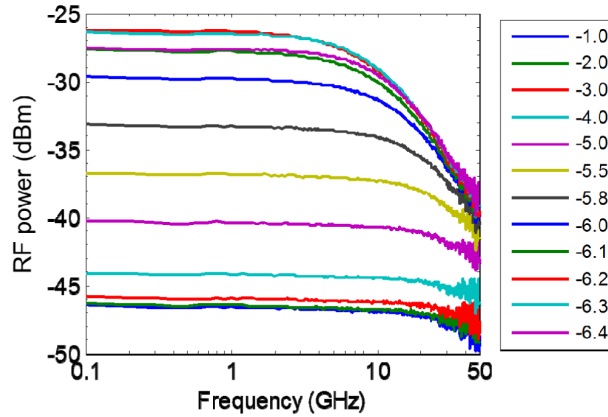

Fig. 3. Small-signal RF measurement of S_{21} parameter for various bias voltages. As the reverse bias is increased beyond −2V, a substantial increase in the S_{21} parameter can be observed up to an optimum bias of −6.3V, after which the S_{21} parameter (and hence the gain) starts to drop instead.
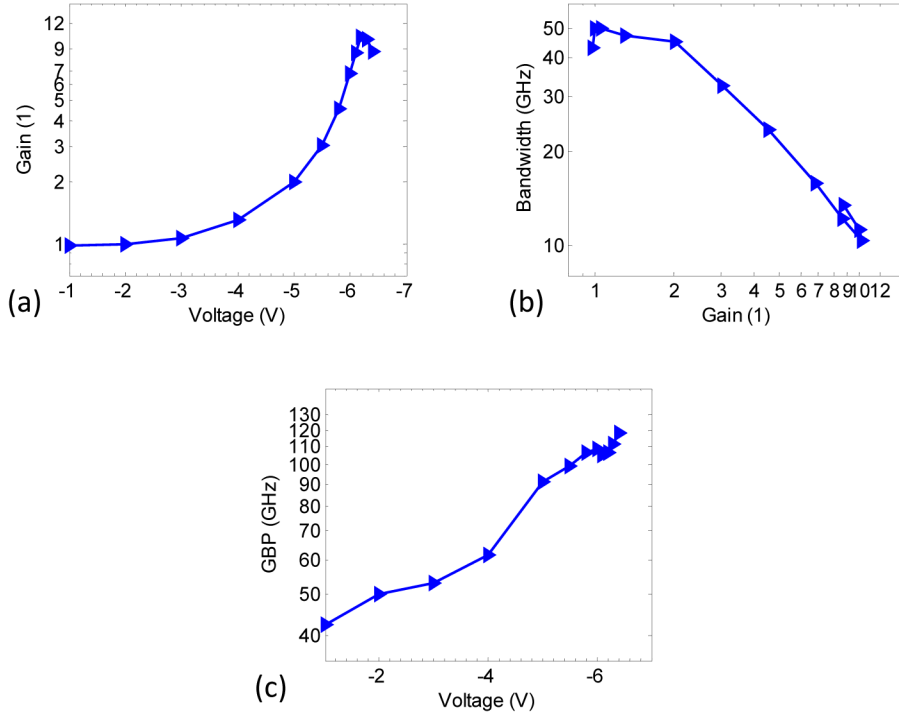

Fig. 4. (a) Avalanche gain extracted from small-signal RF measurements as a function of bias voltage. (b) Measured 3dB opto-electrical bandwidth versus avalanche gain extracted from the S_{21} RF curves. (c) gain × bandwidth product as a function of bias voltage.

3.3 Avalanche excess noise characteristics

Next, excess multiplication noise measurements are performed to characterize the avalanche noise performance of the Ge APDs. The power spectral density (PSD) of the noise current at 150MHz in both dark current and light current were measured using a low-noise signal

analyzer. The power spectral density under consideration (the net-light current power spectral density) is given by Eq. (1) in the avalanche multiplication regime,

$$PSD = 2 \times q \times I \times M^2 \times F(M) \tag{1}$$

where I is net-light current ($=$ light current – dark current) and M is net-light current gain (the avalanche gain extracted from static measurements). q is the elementary charge. The excess noise factor $F(M)$ deduced from Eq. (1) as a function of gain is shown in Fig. 5(a) and Fig. 5(b) at 1550nm wavelength for an input optical power of -23.8dBm and -18.8dBm, respectively. The excess noise factor can be expressed for the case of avalanche multiplication in a uniform electric field when electrons initiate the multiplication as in Eq. (2),

$$F(M) = k_{eff} M + (2 - 1/M) \times (1 - k_{eff}) \tag{2}$$

where k_{eff} is the effective ratio of ionization coefficients for electrons and holes. These ionization coefficients are almost equal in bulk Ge giving a k_{eff} of about 0.9, which results in a very large excess noise, making conventional Ge APDs uncompetitive for building digital optical links. Fitting the data with Eq. (2) reveals a k_{eff} of 0.5 in the presented device. The total reduction of the power spectral density of the noise current in the presented device compared to a bulk Ge APD can be estimated as 35% for an avalanche gain of 10. This is attributed to the dead space effect (the fact that the multiplication region thickness becomes comparable to the distance over which carriers do not experience impact ionization) in the 200nm thin avalanche multiplication region [1, 6, 15–17].
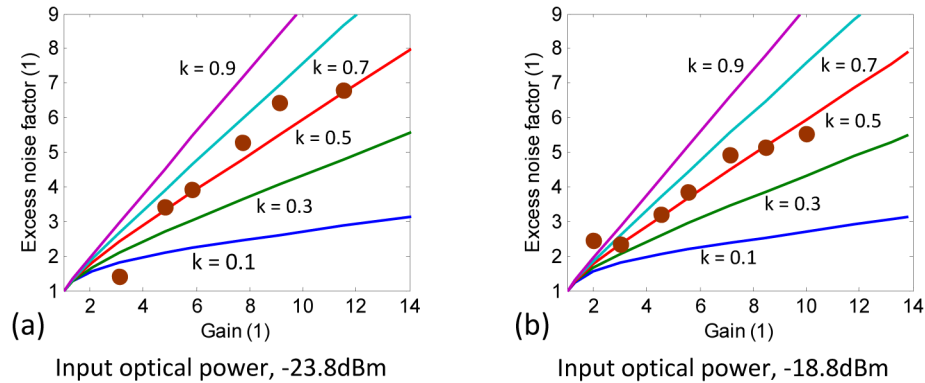

Fig. 5. The excess noise factor as a function of gain with an input optical power of (a) -23.8dBm and (b) -18.8dBm.

The measured k_{eff} of 0.5 in this paper is larger than that of ~0.2 reported in [6]. This can be explained by the fact that the region of impact ionization in germanium is just 30nm as for the MSM structure in [6], while it is ~200nm in the PIN structure demonstrated in this paper. A thinner avalanche region results in more noise reduction effects and thus a smaller k_{eff}.

4. APD receiver characteristics

Finally, in order to assess the sensitivity improvement by operating the APD in avalanche mode, the device was wire-bonded to a 10Gb/s trans-impedance amplifier (TIA), as shown in Fig. 6(a). The TIA is implemented in 0.13μm SiGe BiCMOS technology and has a differential output [10,11]. It is designed for burst-mode operation in access networks with an input referred RMS noise current lower than 1.2μA. A $(2^{31}-1)$ long optical non-return-to-zero pseudo-random bit sequence (PRBS) data pattern at 10Gb/s, generated by a commercial optical modulator with 8.9dB extinction ratio, was launched into the wire-bonded APD

receiver. The eye diagram of the optical signal generated by the modulator is shown in Fig. 6(b). A commercial limiting amplifier (LA) is connected to the TIA, and the LA differential outputs (both the DATA and XDATA port) were fed to a 10Gb/s error detector for bit error ratio (BER) measurement. The measured differential BER as a function of input optical power for various bias voltages are shown in Fig. 7. For a BER of 1×10^{-12} (1×10^{-9}), the waveguide-referred primary sensitivity is −17.6dBm (−18.6dBm) average optical power at −1.7V bias voltage, mostly limited by the TIA input-referred noise (RMS) current. The sensitivity increases with increasing bias. At −5.9V APD bias voltage, a 5.8dB sensitivity improvement is obtained, which yields an absolute receiver sensitivity of −23.4dBm and −24.4dBm for a 1×10^{-12} and 1×10^{-9} BER respectively. The avalanche gain, extracted from the small-signal measurements, is about 6 at −5.9V bias voltage. Beyond −5.9V, while the gain still rises as the bias voltage increases until −6.2V, the sensitivity saturates due to the excess multiplication noise. 10Gb/s eye diagrams of the electrical signals from the LA with differential BER of ~1×10^{-12} at −5.9V bias voltages for both the DATA and XDATA port were recorded by a high-speed oscilloscope, as shown in Fig. 6(c) and Fig. 6(d) respectively.
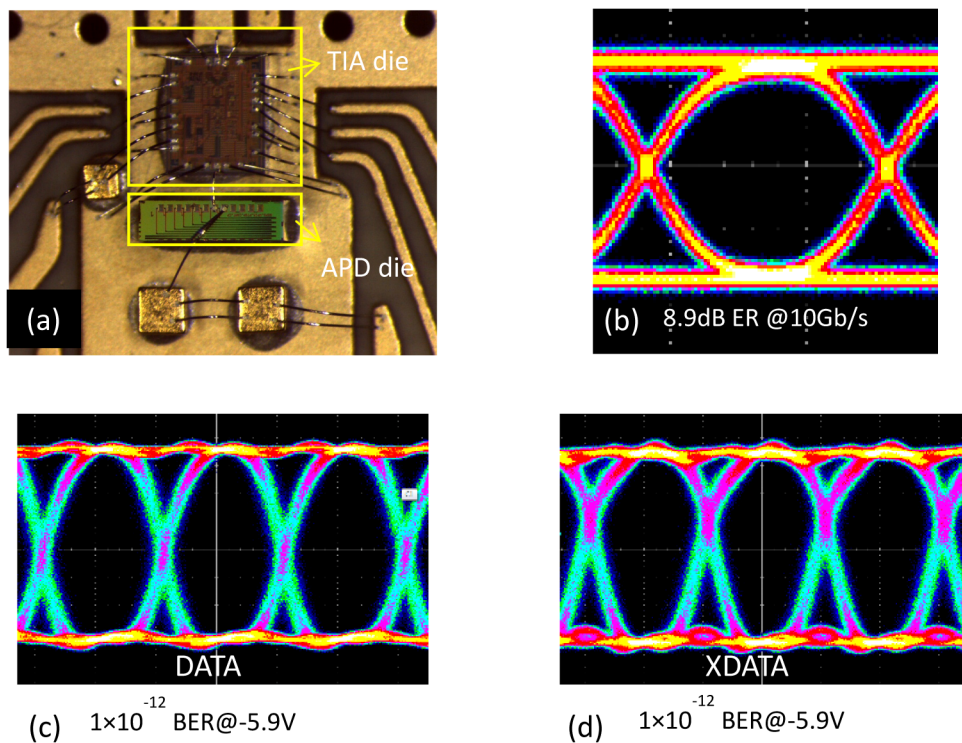

Fig. 6. (a) Optical receiver with Ge APD wire-bonded to a TIA. (b) 10Gb/s optical eye diagram from modulator. (c) 10Gb/s eye diagram of the electrical signal from LA DATA port with differential BER of 1×10^{-12} at −5.9V bias voltage (input optical power is −23.4dBm). (d) 10Gb/s eye diagram of the electrical signal from LA XDATA port with differential BER of 1×10^{-12} at −5.9V bias voltage (input optical power is −23.4dBm).

The sensitivity improvement of 5.8dB is lower than that reported in [8], where the Q factor is used to characterize sensitivity and a 7dB improvement is obtained for a Q factor of 7. This is because the low-noise TIA used in this paper has a much smaller input referred RMS noise current than that of the TIA (implemented in 40nm LP CMOS technology) wire-bonded in [8].
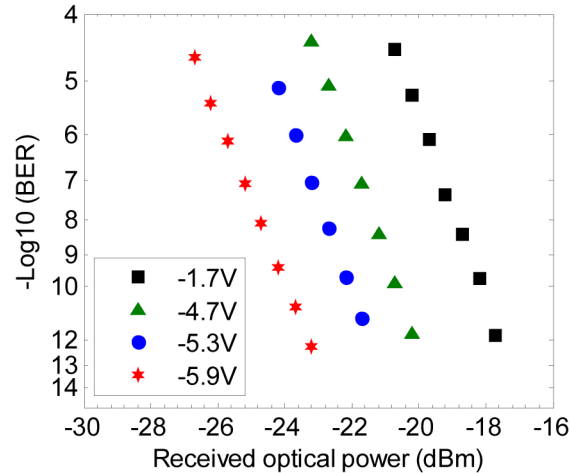
Fig. 7. Measured bit error ratio as a function of input optical power for various bias voltages.

Despite the sensitivity improvement of 5.8dB, both the primary responsivity of 0.6A/W (limited mostly due to the light absorption in the via contacts to the germanium) and the k_{eff} value of 0.5 need to be improved to further increase the absolute sensitivity of the wire-bonded optical receiver, which is −23.4dBm for a 1×10^{-12} BER at 1550nm wavelength in this paper. Compared with a Ge PIN photodetector with state-of-art responsivity of ~1.1A/W [21], assuming a TIA with the same noise performance as that of the TIA used in this paper, the wire-bonded APD-based optical receiver provides ~3dB sensitivity margin over that of the PIN photodetector based optical receiver. Furthermore, a SACM waveguide APD based optical receiver has been demonstrated with −30.4dBm sensitivity for a 1×10^{-12} BER at 1304nm [22] by leveraging the superior avalanche performance of silicon with a k_{eff} of ~0.1. The operation voltage of the SACM waveguide APD is, however, as high as −25V. Increasing primary responsivity and reducing k_{eff} so as to boost the absolute sensitivity of the Ge APD based optical receiver are therefore of key importance for further sensitivity enhancement.

5. Conclusion & outlook

Low-voltage germanium waveguide APDs are demonstrated with a gain × bandwidth product over 100GHz. The optical receiver based on such a Ge APD demonstrates a 5.8dB sensitivity improvement. This can compensate for certain channel insertion loss of optical data links, and thus help to satisfy the required link power budget. In order to further increase the absolute sensitivity of the Ge APD based optical receivers, both the primary responsivity and the effective ratio of ionization coefficients need to be improved.

Acknowledgments